

Dynamic Synchrophasor Estimation with Modified Hybrid Method

Cheng Qian, *Graduate Student Member, IEEE*, Mladen Kezunovic, *Fellow, IEEE*

Dept. of Electrical and Computer Engineering
Texas A&M University, College Station
College Station, TX, US

peterqiancheng@tamu.edu, kezunov@ece.tamu.edu

Abstract—Accuracy of synchrophasor measurements is one of the key issues directing the application of synchrophasor/PMU technologies in both transmission and distribution systems. This paper introduces a dynamic phasor estimation method for PMUs/IEDs based on modified time domain hybrid method. Dynamic phasor is estimated using Taylor expansion, where frequency deviation is derived directly from fitting parameters to avoid magnification of fitting errors. Using the samples from less than 1.2 cycles, the proposed method constructs three windows and then performs recursive DFT on both signal samples and modeled signal for parameter estimation. By scrutinizing the position for time-tagging and approximation, the precision of hybrid method is further improved and the implementation is made easier. This method is essentially rendered immune to harmonics by incorporating DFT in synchrophasor estimation. Performance of the method is investigated through simulations that prove high precision under both static and dynamic signals from real power system scenarios.

Index Terms—Hybrid time domain method, phasor measurement unit, power system measurements, synchrophasor estimation, Smart Grid.

I. INTRODUCTION

Synchrophasor and phasor measurement units (PMUs) are providing a higher resolution for capturing power system disturbances and enabling wide area protection and control schemes, hence serving as a new monitoring and control system that complements EMS in transmission systems [1,2]. Recently, applications of synchrophasor measurement technology (SMT) and PMUs in distribution networks, such as micro-synchrophasors [3], are drawing growing attention and investment [4-6]. Distribution systems are distinct from transmission systems in system topology, the availability and features of measurements, and the exposure to higher level of noise, variations and uncertainties [7]. Consequently, there are more challenges on the application of synchrophasors in distribution networks, and higher accuracy is required for synchrophasor algorithms, PMUs, and PMU-enabled IEDs.

Synchrophasor algorithms proliferate since the inception of SMT. The most basic method is Discrete Fourier Transform (DFT), which models the input signal with nominal frequency sinusoid and its harmonics [8]. Over the years, revisions of traditional DFT method have been developed and can be classified into either time domain method or frequency domain method [9]. Frequency domain methods focus either on the design of high performance digital filters [10], or improvement and compensation of traditional DFT, such as interpolated DFT [11,12]. These methods generally feature heavy involvement of complicated signal processing and filter design techniques. Despite good frequency domain performance, due to the incompatibility between high frequency resolution and short window length, these methods struggle to find the balance between frequency response improvement and limiting transient response time.

On the other hand, time domain methods in generally utilize least square based curve fitting techniques. Therefore, with adequately high sampling frequency that provides enough samples, window length does not significantly affect the performance of time domain methods. The most common time domain methods employ polynomial fitting on either the envelopes of transient power system signal waveforms [13,14], or on complex dynamic phasors [15,16]. Frequency performance of time domain methods is not as good as frequency domain methods since the modeling of envelopes assumes a slow varying process which may not be the best for all scenarios. A hybrid method that creatively incorporates DFT and envelope fitting is introduced in [17]. The method uses the DFT results on three consecutive moving windows for parameter estimation. However, the paper fails to consider accurate time-tagging for DFT results on consecutive moving windows, which consequently increases complexity, and results in systematic error caused by ill-conditioning.

This paper improves the accuracy of hybrid method by scrutinizing the position for time-tagging which is proved theoretically and in simulations. Typically, 1.2 signal cycles are needed to guarantee high accuracy for signals in all steady and dynamic scenarios. Recursive DFT is utilized to simplify

the algorithm. The rest of the paper is organized as follows, Section II presents the interchangeability of the two most commonly used time domain methods. Proposed method is introduced in Section III where rigid theoretical proof is presented. Section IV gives the simulation results for the proposed method. Conclusion is outlined afterwards.

II. TIME DOMAIN METHODS REVISITED

Instead of transforming data samples to another domain (for example, frequency domain in Fourier methods), time domain methods process samples directly in time domain. The basic idea is to utilize simpler functions on a small region of interest to approximate the trigonometric functions which describe power system signals, as shown in (1).

$$x(t) = a(t) \cos(2\pi f_0 t + 2\pi \int \Delta f(t) dt + \varphi_0) \quad (1)$$

where $a(t)$ represents instant amplitude, f_0 is system nominal frequency, Δf is instant frequency deviation, φ_0 is the phase angle at $t = 0$, $\varphi(t) \stackrel{\text{def}}{=} 2\pi \int \Delta f(t) dt + \varphi_0$ denotes the instantaneous phase angle.

The signal in (1) corresponds to the dynamic phasor shown in (2).

$$p(t) = a(t)e^{j\varphi(t)} \quad (2)$$

Equation (2) can be approximated by n th order Taylor expansion around time-tag t_c [14].

$$p(t) = a(t) \cos \varphi(t) + ja(t) \sin \varphi(t) \approx \sum_{i=0}^n d_i (t - t_c)^i \quad (3)$$

where $d_i \stackrel{\text{def}}{=} c_i + js_i = \frac{1}{i!} p^{(i)}(t)$. Therefore,

$$\begin{aligned} x(t) &= a(t) \cos \varphi(t) \cos(2\pi f_0 t) - a(t) \sin \varphi(t) \sin(2\pi f_0 t) \\ &= \mathbf{Re}[p(t)] \cos(2\pi f_0 t) - \mathbf{Im}[p(t)] \sin(2\pi f_0 t) \end{aligned} \quad (4)$$

where $\mathbf{Re}[p(t)] = (p + \hat{p})/2$, $\mathbf{Im}[p(t)] = (p - \hat{p})/2$. \hat{p} denotes the conjugate of p . Therefore,

$$\mathbf{Re}[p(t)] \approx \frac{1}{2} \left[\sum_{i=0}^n d_i (t - t_c)^i + \sum_{i=0}^n \hat{d}_i (t - t_c)^i \right] \quad (4a)$$

$$\mathbf{Im}[p(t)] \approx \frac{1}{2} \left[\sum_{i=0}^n d_i (t - t_c)^i - \sum_{i=0}^n \hat{d}_i (t - t_c)^i \right] \quad (4b)$$

Simplify (4a) and (4b) with $d_i = c_i + js_i$, we have,

$$\mathbf{Re}[p(t)] \approx \sum_{i=0}^n c_i (t - t_c)^i \stackrel{\text{def}}{=} q(t) \quad (5a)$$

$$\mathbf{Im}[p(t)] \approx \sum_{i=0}^n s_i (t - t_c)^i \stackrel{\text{def}}{=} r(t) \quad (5a)$$

Replacing the real and imaginary parts of $p(t)$ in (4), original signal can be represented as,

$$x(t) = q(t) \cos(2\pi f_0 t) - r(t) \sin(2\pi f_0 t) \quad (6)$$

which corresponds to the method in [14]. Therefore, fitting of dynamic phasor and the envelopes of transient waveform are essentially interchangeable through the relationship $d_i = c_i + js_i$.

III. SYNCHROPHASOR ESTIMATION USING MODIFIED HYBRID MEHTOD

Synchrophasor measurement algorithm is a module whose input is an array of samples, and the output only corresponds to one time instant. Therefore, the time-tagging of estimation results unavoidably affects the accuracy of algorithm.

In hybrid method, Taylor polynomials are used to approximate the signal first. To improve the performance of time domain method, DFT is plugged in to alleviate noise and harmonic distortion. Since DFT is essentially an averaging calculation, time-tagging at the center of window, denoted by t_c , will yield the most accurate result. Therefore, expanding the signal at $t_c = N\Delta t/2$, where N is an even number of samples in a window, Δt is the sampling interval. We have DFT for the first window where indices are from 0 to $N-1$,

$$\dot{X}_0 = \sum_{k=0}^{N-1} x(k\Delta t) e^{-j\frac{2\pi}{N}k} \quad (8)$$

where $x(k\Delta t) = q(k\Delta t) \cos\left(\frac{2\pi k}{N}\right) - r(k\Delta t) \sin\left(\frac{2\pi k}{N}\right)$.

Expanding $q(k\Delta t)$ and $r(k\Delta t)$ at $t_c = \frac{N}{2}\Delta t$ using second order Taylor polynomials, we have,

$$\begin{aligned} q(k\Delta t) &\approx c_0 + c_1(k\Delta t - t_c) + c_2(k\Delta t - t_c)^2 \\ &= c_0 + c_1\left(k - \frac{N}{2}\right)\Delta t + c_2\left(k - \frac{N}{2}\right)^2 \Delta t^2 \end{aligned} \quad (9a)$$

$$\begin{aligned} r(k\Delta t) &\approx s_0 + s_1(k\Delta t - t_c) + s_2(k\Delta t - t_c)^2 \\ &= s_0 + s_1\left(k - \frac{N}{2}\right)\Delta t + s_2\left(k - \frac{N}{2}\right)^2 \Delta t^2 \end{aligned} \quad (9b)$$

Substitute $x(k\Delta t)$ with (9a) and (9b), and separate real and imaginary parts of \dot{X}_0 . We have,

$$\begin{aligned} X_{0,Re} &= \mathbf{Re}[\dot{X}_0] \\ &= \sum_{k=0}^{N-1} \left[c_0 + c_1\left(k - \frac{N}{2}\right)\Delta t + c_2\left(k - \frac{N}{2}\right)^2 \Delta t^2 \right] \cos^2 \frac{2\pi k}{N} \\ &\quad - \sum_{k=0}^{N-1} \left[s_0 + s_1\left(k - \frac{N}{2}\right)\Delta t + s_2\left(k - \frac{N}{2}\right)^2 \Delta t^2 \right] \sin \frac{2\pi k}{N} \cos \frac{2\pi k}{N} \end{aligned} \quad (10a)$$

$$\begin{aligned} X_{0,Im} &= \mathbf{Im}[\dot{X}_0] \\ &= -\sum_{k=0}^{N-1} \left[c_0 + c_1\left(k - \frac{N}{2}\right)\Delta t + c_2\left(k - \frac{N}{2}\right)^2 \Delta t^2 \right] \sin \frac{2\pi k}{N} \cos \frac{2\pi k}{N} \\ &\quad + \sum_{k=0}^{N-1} \left[s_0 + s_1\left(k - \frac{N}{2}\right)\Delta t + s_2\left(k - \frac{N}{2}\right)^2 \Delta t^2 \right] \sin^2 \frac{2\pi k}{N} \end{aligned} \quad (10b)$$

Organize (10) in the form of parameters of c_i and s_i , as shown in (11) on the top of next page.

Thus we have two knowns (real and imaginary parts of DFT) and six unknowns (c_i and s_i). In order to balance the number of knowns and unknowns, three equally spaced windows are utilized, and the original signal is approximated at t_c , $t_c + \Delta t$, $t_c + 2\Delta t$, respectively. The assumption is that the fitting coefficients do not change when utilizing data from moving windows, which is reasonable since the typical sampling rate for a PMU is 2880Hz (48 samples/cycle) whereas the transient of envelopes is a few Hz, thus the fitting error is negligible. Use of moving windows is shown in Figure 1. Mechanism of hybrid method is illustrated in Figure 2.

$$X_{0,Re} = c_0 \sum_{k=0}^{N-1} \cos^2 \frac{2\pi k}{N} + c_1 \sum_{k=0}^{N-1} \left(k - \frac{N}{2}\right) \Delta t \cdot \cos^2 \frac{2\pi k}{N} + c_2 \sum_{k=0}^{N-1} \left(k - \frac{N}{2}\right)^2 \Delta t^2 \cdot \cos^2 \frac{2\pi k}{N} - s_0 \sum_{k=0}^{N-1} \sin \frac{2\pi k}{N} \cos \frac{2\pi k}{N} - s_1 \sum_{k=0}^{N-1} \left(k - \frac{N}{2}\right) \Delta t \cdot \sin \frac{2\pi k}{N} \cos \frac{2\pi k}{N} - s_2 \sum_{k=0}^{N-1} \left(k - \frac{N}{2}\right)^2 \Delta t^2 \cdot \sin \frac{2\pi k}{N} \cos \frac{2\pi k}{N} = \alpha_0^0 c_0 + \alpha_1^0 c_1 + \alpha_2^0 c_2 + \lambda_0^0 s_0 + \lambda_1^0 s_1 + \lambda_2^0 s_2 \quad (11a)$$

$$X_{0,Im} = c_0 \sum_{k=0}^{N-1} \sin \frac{2\pi k}{N} \cos \frac{2\pi k}{N} - c_1 \sum_{k=0}^{N-1} \left(k - \frac{N}{2}\right) \Delta t \cdot \sin \frac{2\pi k}{N} \cos \frac{2\pi k}{N} - c_2 \sum_{k=0}^{N-1} \left(k - \frac{N}{2}\right)^2 \Delta t^2 \cdot \sin \frac{2\pi k}{N} \cos \frac{2\pi k}{N} + s_0 \sum_{k=0}^{N-1} \cos^2 \frac{2\pi k}{N} + s_1 \sum_{k=0}^{N-1} \left(k - \frac{N}{2}\right) \Delta t \cdot \cos^2 \frac{2\pi k}{N} + s_2 \sum_{k=0}^{N-1} \left(k - \frac{N}{2}\right)^2 \Delta t^2 \cdot \cos^2 \frac{2\pi k}{N} = \lambda_0^0 c_0 + \lambda_1^0 c_1 + \lambda_2^0 c_2 + \beta_0^0 s_0 + \beta_1^0 s_1 + \beta_2^0 s_2 \quad (11b)$$

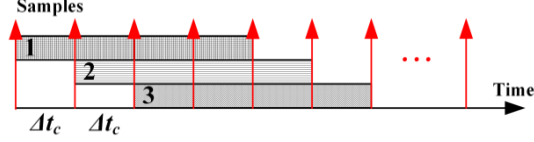


Figure 1. Illustration of Moving Windows

For the second window, where the sample indices are from 1 to N , and we have DFT,

$$\dot{X}_1 = \sum_{k=0}^{N-1} x[(k+1)\Delta t] e^{-i\frac{2\pi}{N}k} = \sum_{k=1}^N x(k\Delta t) e^{-i\frac{2\pi}{N}(k-1)} \quad (12)$$

Or equivalently,

$$\dot{X}_1 e^{-i\frac{2\pi}{N}} = \sum_{k=1}^N x(k\Delta t) e^{-i\frac{2\pi}{N}k} \quad (13)$$

Similarly, for the third window, where the sample indices are from 2 to $N+1$, and we have DFT,

$$\dot{X}_1 e^{-i\frac{2\pi}{N} \cdot 2} = \sum_{k=2}^{N+1} x(k\Delta t) e^{-i\frac{2\pi}{N}k} \quad (14)$$

The rest of the derivation is similar to (10) and (11). Note that the left-hand sides of (13) and (14) correspond to recursive DFT, where the instant phase angle of sinusoid with nominal frequency is considered as the reference angle. Recursive DFT is essentially an angle adjustment, which can be done conveniently in practice. The right-hand sides of (13) and (14) have the same structure as (8), and the only difference is the indices of summation, which does not increase any computation complexity. Otherwise, as discussed in [17], the derived fitting coefficients are irregular and harder to be implemented sustainably when higher order Taylor expansion needs to be considered.

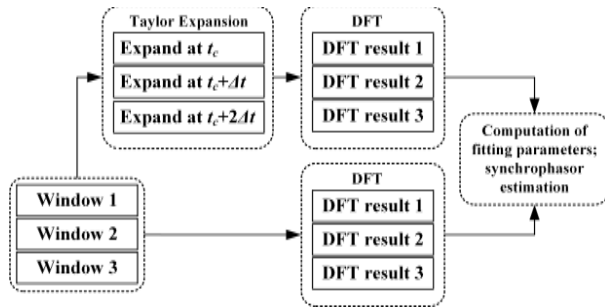


Figure 2. Mechanism of Modified Hybrid Method

In general, the fitting coefficients can be computed as follows:

$$\alpha_m^n = \sum_{k=n}^{N+n-1} \left(k - \frac{N}{2}\right)^m \Delta t^m \cos^m \frac{2\pi k}{N} \quad (15a)$$

$$\beta_m^n = \sum_{k=n}^{N+n-1} \left(k - \frac{N}{2}\right)^m \Delta t^m \sin^m \frac{2\pi k}{N} \quad (15b)$$

$$\lambda_m^n = -\sum_{k=n}^{N+n-1} \left(k - \frac{N}{2}\right)^m \Delta t^m \sin \frac{2\pi k}{N} \cos \frac{2\pi k}{N} \quad (15c)$$

where $m, n = 0, 1, 2, \dots$, the superscript on coefficient denotes the number of windows, and the subscript indicates the order of corresponding polynomial. In order to construct a solvable matrix equation, $\max(m) = \max(n)$ needs to be satisfied.

In the case where $\max(m) = \max(n) = 2$, the matrix equation is as follows,

$$\begin{bmatrix} \mathbf{Re}[\dot{X}_0] \\ \mathbf{Re}[\dot{X}_1 \theta] \\ \mathbf{Re}[\dot{X}_2 \theta^2] \\ \mathbf{Im}[\dot{X}_0] \\ \mathbf{Im}[\dot{X}_1 \theta] \\ \mathbf{Im}[\dot{X}_2 \theta^2] \end{bmatrix} = \begin{bmatrix} \alpha_0^0 & \alpha_1^0 & \alpha_2^0 & \lambda_0^0 & \lambda_1^0 & \lambda_2^0 \\ \alpha_1^0 & \alpha_1^1 & \alpha_2^1 & \lambda_1^0 & \lambda_1^1 & \lambda_2^1 \\ \alpha_2^0 & \alpha_2^1 & \alpha_2^2 & \lambda_2^0 & \lambda_2^1 & \lambda_2^2 \\ \beta_0^0 & \beta_1^0 & \beta_2^0 & \beta_0^0 & \beta_1^0 & \beta_2^0 \\ \beta_1^0 & \beta_1^1 & \beta_2^1 & \beta_1^0 & \beta_1^1 & \beta_2^1 \\ \beta_2^0 & \beta_2^1 & \beta_2^2 & \beta_2^0 & \beta_2^1 & \beta_2^2 \end{bmatrix} \begin{bmatrix} c_0 \\ c_1 \\ c_2 \\ s_0 \\ s_1 \\ s_2 \end{bmatrix} \quad (16)$$

where $\theta \equiv e^{-i\frac{2\pi}{N}}$ is the rotating factor which does not change the amplitude of the phasor and rotate the phase angle clockwise by one sampling angle interval. Note that (16) is a linear matrix equation, where the matrix on the right-hand side is fixed, whose inverse can be calculated and stored beforehand. As a result, solving the fitting coefficient is just a matrix multiplication.

Traditionally frequency is calculated using the differentiation of consecutive angle values. This method may perform well under simulation conditions with noiseless test signals. However, when noise is presented in real measurements, differentiation will inevitably magnify computation uncertainties. Averaging may be applied to smooth raw angle estimations to alleviate error caused by random fluctuation. However, averaging applies on multiple estimation results and thus essentially increases the length of data window. This will adversely affect the transient performance of the algorithm by adding transient time. Moreover, averaging will shift the time-tags of frequency and ROCOF estimation, which are originally aligned with estimated synchrophasors. As a result, time delays will be introduced. In this paper, two matrices are constructed for frequency deviation and ROCOF estimation using acquired fitting coefficients.

Taking the derivative of $p(t) = a(t)e^{j\varphi(t)}$,

$$p'(t) = a'(t)e^{j\varphi(t)} + jp(t)\varphi'(t) \quad (17)$$

Separating real part and imaginary part of (17), we have,

$$\text{Re}[p'(t)] = a'(t) \cos\varphi(t) - s(t) \varphi'(t) = c_1 \quad (18a)$$

$$\text{Im}[p'(t)] = a'(t) \sin\varphi(t) + c(t) \varphi'(t) = s_1 \quad (18b)$$

Or equivalently,

$$\begin{bmatrix} c_1 \\ s_1 \end{bmatrix} = \begin{bmatrix} \cos\varphi(t) & -s_0 \\ \sin\varphi(t) & c_0 \end{bmatrix} \begin{bmatrix} a'(t) \\ \varphi'(t) \end{bmatrix} \quad (19)$$

Solving (19), we have $\varphi'(t) = 2\pi\Delta f(t)$, the estimation is on frequency deviation instead of frequency since recursive DFT is used in the calculation of parameters. Therefore,

$$\Delta f(t) = \frac{\varphi'(t)}{2\pi} \quad (20)$$

Similarly, ROCOF estimation can be performed. Taking the derivative of (17), we have

$$p''(t) = c_2 + js_2 = a''(t) e^{j\varphi(t)} + a'(t) [e^{j\varphi(t)} j\varphi'(t)] + j[p'(t)\varphi'(t) + p(t)\varphi''(t)] \quad (21)$$

Separating real part and imaginary part of (21) and organize into matrix form,

$$\begin{bmatrix} c_2 + a'(t)\varphi'(t)\sin\varphi(t) + s_1\varphi'(t) \\ s_2 - a'(t)\varphi'(t)\cos\varphi(t) - c_1\varphi'(t) \end{bmatrix} = \begin{bmatrix} \cos\varphi(t) & -s_0 \\ \sin\varphi(t) & c_0 \end{bmatrix} \begin{bmatrix} a''(t) \\ \varphi''(t) \end{bmatrix} \quad (22)$$

Note that all parameters except $a''(t)$ and $\varphi''(t)$ have been calculated in (22). Solving (22) we can acquire $\varphi''(t)$. Then ROCOF can be achieved by

$$R_f(t) = \frac{\varphi''(t)}{2\pi} \quad (20)$$

As discussed above, estimated values all have the same time-tag, which is the center of the first window.

IV. SIMULATION STUDIES AND ANALYSIS

A. Test Conditions

All the tests are performed in MATLAB software. Test scenarios are selected from [18], elaborated in Table 1, which include both static and dynamic tests. White Gaussian noise (WGN) is added to imitate the noise from digitization [19]. Sampling frequency is 6kHz.

TABLE I. TEST SCENARIOS IN ALGORITHM TESTS

Test Types		
Static Tests	Signal magnitude range	Signal frequency range
	Harmonic distortion & Out-of-band interference	Phase angle range
Dynamic Tests	Amplitude modulation	Phase modulation
	Amplitude and phase combined modulation	Frequency ramp

The proposed algorithm is tested and compared with the time domain method in [14] and IEEE standard [18]. In [14],

a time domain method based on second order Taylor polynomial expansion alone is utilized to estimate dynamic waveforms. One should note that the method in [14] is originally designed for transient signals with slow varying envelopes. The performance of the proposed algorithm is also tested against the highest accuracy requirements from IEEE Standards for each test type, irrespective of the class of PMU.

Test parameters are specified in Table II. Since theoretically modified hybrid method is immune to harmonics, therefore, in harmonic tests and out-of-band interference test, the system frequency is chosen to be 60.02Hz, instead of nominal frequency. The selection of typical system frequency is based on the observation from [20].

TABLE II. CONDITIONS AND PARAMETERS OF TEST SIGNALS

Test Type	Test Conditions/Parameters
Amplitude deviation	10% rated and 120% rated
Frequency deviation	$\pm 5\text{Hz}$
Angle deviation	$\pm\pi$ rad
Harmonic and out-of-band tests	System frequency at 60.02Hz, 10% harmonics up to 50 th .
Frequency ramp test	$\pm 1\text{Hz/s}$ frequency ramp
Modulation test	10% amplitude and angle combined test, modulation frequency at 5Hz.

All test parameters are chosen to represent the most adverse conditions. Note that some of the tests, for example, amplitude and angle combined test, are not specified in the standards, but exert even higher requirement on algorithm accuracy.

B. TVE and Phase Angle Estimation Results and Analysis

As shown in Table III, the proposed modified hybrid method presents excellent performance in static PMU tests specified in IEEE standards, while traditional Taylor expansion method is susceptible to harmonics and noise. As expected from the theoretical derivation, the hybrid method excels at harmonic and noise rejection.

TABLE III. TVE ESTIMATION ACCURACY

Test Type	IEEE Std.	Modified Hybrid	Taylor Expansion
Steady-state test	1%	0.05%	>10%
Harmonic test	1%	10^{-6}	>10%
OOB test	1.3%	10^{-6}	>10%
Frequency ramp test	1%	0.15%	>10%
Modulation test	3%	0.08%	0.2%

TABLE IV. PHASE ANGLE ESTIMATION ACCURACY

Test Type	IEEE Std. ^[note]	Modified Hybrid	Taylor Expansion
Steady-state test	0.573°	$3 \times 10^{-5^\circ}$	$5 \times 10^{-3^\circ}$
Harmonic test	0.573°	$5 \times 10^{-10^\circ}$	$>1^\circ$
OOB test	0.745°	$5 \times 10^{-10^\circ}$	$>1^\circ$
Frequency ramp test	0.573°	$1.5 \times 10^{-5^\circ}$	$4 \times 10^{-3^\circ}$
Modulation test	1.719°	$8 \times 10^{-6^\circ}$	$8 \times 10^{-4^\circ}$

Note: IEEE does not have separate requirement for phase angle estimation, in this Table amplitude estimation is assumed to be accurate.

Conclusion can be drawn from Table IV that the proposed method has extraordinary phase angle measurement accuracy. This is of particular significance for the Smart Grid,

especially for the promotion and application of synchrophasor technology in distribution networks, where much higher phase angle estimation accuracy is desired since the angle difference between nodes is typically smaller than 0.1°/mile at full load, as compared to tens of degrees in transmission systems[7].

C. Frequency and ROCOF Estimation Results and Analysis

As can be proved from Table V and Table VI, since frequency and ROCOF are derived directly from fitting coefficients, the estimation of those quantities has the same accuracy level as amplitude and phase angle. Whereas in traditional Taylor expansion method, the estimation noise of phase angle is magnified through taking derivatives.

TABLE V. FREQUENCY ESTIMATION ACCURACY

Test Type	IEEE Std.	Modified Hybrid	Taylor Expansion
Steady-state test	0.005Hz	4×10^{-5} Hz	0.35Hz
Harmonic test	0.05Hz	3×10^{-9} Hz	>1Hz
OOB test	0.05Hz	3×10^{-9} Hz	>1Hz
Frequency ramp test	0.01Hz	5×10^{-4} Hz	0.35Hz
Modulation test	0.06Hz	4×10^{-4} Hz	0.05Hz

TABLE VI. ROCOF ESTIMATION ACCURACY

Test Type	IEEE Std.	Modified Hybrid	Taylor Expansion
Steady-state test	0.1Hz/s	3×10^{-4} Hz/s	>1Hz/s
Harmonic test	0.4 Hz/s	8×10^{-8} Hz/s	
OOB test	0.4Hz/s	8×10^{-8} Hz/s	
Frequency ramp test	0.2Hz/s	4×10^{-4} Hz/s	8Hz/s
Modulation test	2Hz/s	5×10^{-4} Hz/s	

V. CONCLUSION

In this paper, a modified hybrid method for dynamic synchrophasor estimation is presented. The proposed method has the merits from both time domain method and Fourier method. The conclusions are as follows.

- The paper proves that the time domain methods that utilize curve fitting on dynamic phasor and envelope of transient waveforms are theoretically interchangeable.
- Taylor expansion is used to approximate dynamic waveforms. DFT is then performed on the model to achieve better frequency domain performance. Frequency and ROCOF are derived directly from fitting coefficients, avoiding introducing error from differentiation of phase angles.
- By scrutinizing the position for Taylor approximation, the original hybrid method in [17] is modified and the estimation error is minimized. Polynomial approximation is performed at the center of each sample window where DFT is the most accurate.
- Recursive DFT is used to simplify parameter estimation. The modified algorithm is adaptable and sustainable when higher order of polynomial expansion and digital filter/window function are to be applied.
- Simulation results confirm that the modified method exhibits high accuracy under both static and dynamic power system signal input. Higher order polynomials can be applied to achieve even higher accuracy.

REFERENCES

- [1]. Synchrophasor Applications in Transmission Systems. [Online]. Available: https://www.smartgrid.gov/recovery_act/program_impacts/applications_synchrophasor_technology.html
- [2]. A. Silverstein and J. E. Dagle, "Successes and Challenges for Synchrophasor Technology: An Update from the North American Synchrophasor Initiative," System Science (HICSS), 2012 45th Hawaii International Conference on, Maui, HI, 2012, pp. 2091-2095.
- [3]. A. von Meier, D. Culler, A. McEachern and R. Arghandeh, "Micro-synchrophasors for distribution systems," Innovative Smart Grid Technologies Conference (ISGT), 2014 IEEE PES, Washington, DC, 2014, pp. 1-5
- [4]. M. Wache and D. C. Murray, "Application of Synchrophasor Measurements for distribution networks," Power and Energy Society General Meeting, 2011 IEEE, San Diego, CA, 2011, pp. 1-4.
- [5]. G. Hataway, B. Flerhinger, R. Moxley, Synchrophasors for Distribution Applications. [Online]. Available: https://cdn.selinc.com/assets/Literature/Publications/Technical%20Papers/6561_SynchrophasorsDistribution_RM_20121030_Web.pdf
- [6]. A. von Meier, D. Culler, A. McEachern and R. Arghandeh, Micro-synchrophasors for distribution systems, Innovative Smart Grid Technologies Conference (ISGT), 2014 IEEE PES, Washington, DC, 2014, pp. 1-5. [Online]. Available: <http://arxiv.org/abs/1408.1736>
- [7]. A. von Meier, R. Arghandeh, Every Moment Counts: Synchrophasors for Distribution Networks with Variable Resources. [Online]. Available: <http://arxiv.org/ftp/arxiv/papers/1408/1408.1736.pdf>
- [8]. A. G. Phadke, J. S. Thorp, and M. G. Adamiak, "A new measurement technique for tracking voltage phasors, local system frequency, and rate of change of frequency," *IEEE Trans. Power Apparatus and Systems*, vol. 102, pp. 1025-1038, May 1983
- [9]. C. Qian, T. Bi, J. Li, H. Liu, and Z. Liu, "Synchrophasor estimation algorithm using Legendre polynomials," PES General Meeting | Conference & Exposition, 2014 IEEE, vol., no., pp. 1-5, 27-31 July 2014.
- [10]. D. Macii, G. Barchi, D. Petri, "Design criteria of digital filters for synchrophasor estimation," Instrumentation and Measurement Technology Conference (I2MTC), 2013 IEEE International , vol., no., pp.1579,1584, 6-9 May 2013
- [11]. P. Romano, M. Paolone, "Enhanced Interpolated-DFT for Synchrophasor Estimation in FPGAs: Theory, Implementation, and Validation of a PMU Prototype," Instrumentation and Measurement, IEEE Transactions on , vol.63, no.12, pp.2824,2836, Dec. 2014.
- [12]. T. Bi, H. Liu, Q. Feng, C. Qian, and Y. Liu, "Dynamic Phasor Model-Based Synchrophasor Estimation Algorithm for M-Class PMU," *IEEE Trans. Power Delivery*, vol.30, no.3, pp.1162-1171, June 2015.
- [13]. R. Mai, Z. He, L. Fu; B. Kirby, Z. Bo, "A Dynamic Synchrophasor Estimation Algorithm for Online Application," Power Delivery, IEEE Transactions on , vol.25, no.2, pp.570,578, April 2010
- [14]. J. Ren, and M. Kezunovic, "An Adaptive Phasor Estimator for Power System Waveforms Containing Transients," *IEEE Trans. Power Delivery*, vol.27, no.2, pp.735,745, April 2012.
- [15]. J.A.d. de la Serna, "Dynamic Phasor Estimates for Power System Oscillations," Instrumentation and Measurement, IEEE Transactions on , vol.56, no.5, pp.1648,1657, Oct. 2007
- [16]. Premerlani, W.; Kasztenny, B.; Adamiak, M., "Development and Implementation of a Synchrophasor Estimator Capable of Measurements Under Dynamic Conditions," Power Delivery, IEEE Transactions on , vol.23, no.1, pp.109,123, Jan. 2008
- [17]. J. Ren and M. Kezunovic, "A Hybrid Method for Power System Frequency Estimation," in IEEE Transactions on Power Delivery, vol. 27, no. 3, pp. 1252-1259, July 2012.
- [18]. A. Goldstein, et al., IEEE Synchrophasor Measurement Test Suite Specification. New York: IEEE, 2014
- [19]. C. Qian, M. Kezunovic, "Synchrophasor Reference Algorithm for PMU Calibration System," PES Transmission and Distribution (T&D) Conference and Exposition, in press.
- [20]. FNET/GridEye Web Display. [Online]. Available: <http://fnetpublic.utk.edu/gradientmap.html>